Journal of Atmospheric and Solar-Terrestrial Physics 72 (2010) 1299–1308

Contents lists available at ScienceDirect

Journal of Atmospheric and Solar-Terrestrial Physics

journal homepage: www.elsevier.com/locate/jastp

Ionospheric effects near the magnetic equator and the anomaly crest of the Indian longitude zone during a large number of intense geomagnetic storms

R. Hajra [a], S.K. Chakraborty [a,*], A. DasGupta [b]

[a] Department of Physics, Raja Peary Mohan College, Uttarpara, Hooghly 712258, India
[b] S. K. Mitra Center for Research in Space Environment, University of Calcutta, Calcutta 700009, India

ARTICLE INFO

Article history:
Received 27 May 2010
Received in revised form
15 August 2010
Accepted 9 September 2010
Available online 18 September 2010

Keywords:
Ionosphere (Equatorial ionosphere, Ionospheric disturbances, Ionospheric irregularities, Ionospheric storms)

ABSTRACT

Ionospheric effects of a large number (51) of severe geomagnetic storms are studied using total electron content (TEC) and VHF/UHF scintillation data from Calcutta, situated near the northern crest of equatorial ionization anomaly and equatorial spread-F (ESF) data from Kodaikanal. The susceptibility of the equatorial ionosphere to develop storm time plasma density irregularities responsible for ESF and scintillation is found to be largely modulated by the local times of occurrences of main and recovery phases as seen in the D_{st} index. While inhibition of premidnight scintillation for lower TEC values compared to the quiet day averages is omnipresent, occurrence of scintillation for enhancements of TEC is largely dependent on initiation time and amplitude of the said deviations. An overall reduction in threshold values of h′F for observing storm induced ESF and scintillation compared to reported quiet time values is noted. The results are discussed in terms of storm time variabilities in electric fields, neutral wind system and composition changes.

1. Introduction

The two most important features of the equatorial ionosphere are the equatorial ionization anomaly (EIA) and the intense form of plasma density irregularities. The study of the phenomenon of plasma density irregularities which often characterize the equatorial F-region at night is important for maintenance of fail-safe transionospheric communication and navigation links. The development along with different aspects of the irregularities, like temporal, seasonal, solar activity and longitude dependences are well documented using theoretical study (Sultan, 1996, and references therein) as well as multi-technique studies based on (i) bottomside spread echoes in the ionograms (Cohen and Bowles, 1961; Woodman and LaHoz, 1976), (ii) scintillations of radio waves in the frequency range 100 MHz–4 GHz (Basu et al., 2002, and references therein), (iii) thermospheric airglow intensity bite-outs (Weber et al., 1983; Sahai et al., 2004), (iv) plume-like structures in radar maps (Kelley et al., 1981), etc. However, the day-to-day and storm time variability patterns of the irregularities are not well understood even after several decades of investigation.

The plasma density irregularities are generated due to ionospheric instability (Rayleigh–Taylor instability) driven by eastward equatorial electric field and wind system under the suitable conditions of Pedersen conductivity and upward electron density gradient (Haerendel, 1973; Anderson and Haerendel, 1979; Haerendel et al., 1992; Sultan, 1996; Abdu et al., 2009). The magnetosphere–ionosphere coupling during severe geomagnetic storms leads to intricate modifications of equatorial electric fields, thermospheric wind system and, in turn, the background ionospheric properties like conductivities and ambient electron density. The drastic modifications of the stated parameters may develop unpredictable changes to the quiet time climatological patterns of the irregularities, which may be tracked by scintillation and equatorial spread-F (ESF) techniques.

A large volume of case and a few statistical studies on storm time evolution of irregularities, now available, may lead to the generalized conclusion that the quite time morphology of irregularities is mostly reversed during the period of geomagnetic disturbances. Under quite geomagnetic conditions the irregularities are mainly premidnight phenomena occurring frequently during high solar activity years with seasonal pattern dependent on longitude sectors (Kil and Heelis, 1998; McClure et al., 1998; Su et al., 2008). However, during the periods of geomagnetic disturbances (i) the occurrence probability of premidnight events is reported to decrease during "ESF seasons" and increase during "non-ESF seasons", (ii) the occurrences of postmidnight events increase during each season (Chandra et al., 1979; Rastogi et al., 1981; Groves et al., 1997; Becker-Guedes et al., 2004) and (iii) the irregularities are suppressed near solar maximum and enhanced

* Corresponding author. Tel.: +91 33 2664 9178.
E-mail address: skchak2003@yahoo.com (S.K. Chakraborty).

1364-6826/$ - see front matter © 2010 Elsevier Ltd. All rights reserved.
doi:10.1016/j.jastp.2010.09.015

in postmidnight periods of low solar activity years (Fejer et al., 1999; Hysell and Burcham, 2002).

The study of DasGupta et al. (1985) indicated the importance of severity as well as the local times of peak development of the storms (in terms of D_{st}) for triggering of equatorial irregularities. Several statistical and case studies thereafter (Dabas et al., 1989; Aarons, 1991; Basu et al., 2001; Biktash, 2004; Kumar et al., 2005) explored the significance of the local times of maximum ring current intensification and phases of the storms in dictating the presence or absence of irregularities. In the main phase of the storms, irregularities during local postsunset hours were reported to be triggered by the action of magnetospheric dynamo in the longitude sectors for which local dusk time corresponds to the time of rapid decreases in D_{st} index (Basu et al., 2001, 2005; Huang et al., 2002) and/or sudden increases in AE index (Tulasi Ram et al., 2008). Using the equatorial disturbance plasma drift model proposed by Fejer and Scherliess (1995, 1997) and Scherliess and Fejer (1997), Martinis et al. (2005) attempted a synthesis of the equatorial irregularity processes. Accordingly, the variability of premidnight events was attributed to the variability of prereversal enhancement (PRE) of equatorial upward plasma drifts instigated by the relative dominance of magnetospheric or ionospheric disturbance dynamos. On the other hand, the enhanced generation of the postmidnight events was suggested to be related to the anomalous reversal of the nighttime equatorial drifts from downward to upward direction by the action of ionospheric disturbance dynamo. Seasonal, solar activity and nocturnal (pre or postmidnight occurrences) dependences of the geomagnetic activity control on the irregularity processes were suggested to be related to the corresponding response of the equatorial vertical plasma drifts (Fejer et al., 1999; Martinis et al., 2005). More recent studies (Burke et al., 2009, and references therein) based on the topside observations by DMSP spacecraft at $\sim$850 km altitude reported prolonged absence of premidnight irregularities during the recovery phase. The absence is attributed to the reduction in the amplitude of PRE by the modified wind dynamics, chemical composition and plasma density.

Inspite of large number of case studies and a few morphological studies on the storm related changes of various ionospheric parameters, the understanding of the variability of the ionosphere in the low latitude region, particularly near the EIA crest, during geomagnetic disturbances have not reached a level such that development of a model in the context of variability of ambient ionization and generation of equatorial irregularities/occurrence of scintillation is possible. This necessitates augmentation of knowledge concerning storm related variabilities of several ionospheric parameters for which studies based on an appreciable number of storm events are essential.

In the present investigation, ESF recorded at an equatorial station Kodaikanal (geographic: longitude 77.5°E, latitude 10.25°N, dip: 4°N), total electron content (TEC) and VHF/UHF scintillations observed at Calcutta (geographic: longitude 88.38°E, latitude 22.58°N, dip: 32°N) are extensively studied during periods of a large number (51) of severe geomagnetic storms ($D_{st} \leq -100$ nT) distributed over a solar cycle (1980–1990). The observing station Calcutta is situated near the northern crest of EIA. World's largest values of ionization are observed around the anomaly crest location. For the same percentage variation of ionization density at the equatorial region the largest amplitudes of deviations are observed around the crest, favoring intense scintillation activity at night.

Among the various schemes available to characterize the effects of geomagnetic disturbances, phases of storms (main or recovery) and the corresponding local times of onset seem to play important roles in dictating the ionospheric changes. The storms are classified according to the local times of main phase onset (MPO) and end of main phase (EMP). The study of the phenomena of ESF and scintillations, separated on the basis of their occurrences in pre or postmidnight sectors during the nights pertaining to different phases of the storms with respective local times of initiations, helps to develop the morphological pattern of the equatorial irregularities in the context of the temporal evolution of the main and recovery phases of the storms.

2. Data

Ionospheric TEC data analyzed for the present investigation are obtained through the technique of Faraday rotation of plane polarized VHF (136.11 MHz) signal from geostationary satellite ETS-2 (130°E) recorded at the Ionosphere Field Station, Haringhata, University of Calcutta, located around the northern crest of the EIA.

For amplitude scintillations, VHF (136.11 MHz) and UHF (244 MHz) transmissions from two satellites ETS-2 and Fleet Sat Com (FSC) (73°E) are used. The 400 km sub-ionospheric point of ETS-2 is located at 21°N, 92.7°E (geographic), dip: 27°N and that of FSC is at 21.1°N, 87.1°E (geographic), dip: 27°N. Scintillations above 6 dB level (i.e., moderate and saturated scintillations) associated with F-region irregularities are considered for the present investigation. F-region scintillation at VHF/UHF is generally quite fast and saturated within a few minutes. E-region scintillation is slowly varying with quasi-periodic fluctuations at the beginning/start and end. The presence of scintillation at any satellite path is counted for the statistical analysis. Ionosonde data, available at 1 h interval, from the equatorial station Kodaikanal are used for information regarding ESF and virtual height of F-layer (h′F). The parameters are scaled manually.

Only the intense geomagnetic storm events with $D_{st} \leq -100$ nT (Sugiura and Chapman, 1960) are considered for the present investigation. The total number of storms studied is 51. Though the actual number of severe geomagnetic storms during the period (1980–1990) of investigation is more than 100, the number of events investigated is less due to non-availability of simultaneous scintillation and TEC data during satellite eclipse periods and equipment failures. The consecutive severe storm events separated with a time gap of about one/two days are not taken in account as the effects of independent events with clear main and recovery phases are only considered for the present study. Among the storms considered 83% are of sudden commencement type and the rest of gradual commencement type.

The occurrence patterns of irregularities in the main and recovery phases of the geomagnetic storms are studied separately. All the storm events are grouped into three categories according to the local times of MPO and EMP. These are storms with MPO/EMP during (i) daytime (0530–1730 h IST)—Category 1, (ii) premidnight (1830–2330 h IST)—Category 2 and (iii) postmidnight (0030–0430 h IST)—Category 3. IST stands for Indian standard time (=UT+0530 h). Fig. 1 shows the distribution of the studied storm events for each local time sector of MPO and separated on the seasonal basis, i.e., local winter (November, December and January), summer (May, June and July) and equinoxes (February, March, April, August, September and October).

D_{st} index, used for severity of the geomagnetic storms, are downloaded from the website of the World Data Centre for Geomagnetism, Kyoto (http://wdc.kugi.kyoto-u.ac.jp/). The interplanetary magnetic field component (IMF B_z) available with the website of the NOAA's National Geophysical Data Centre, Boulder (http://www.ngdc.noaa.gov/) are used in the present study. For solar flux, $F_{10.7}$ data available with the website (http://www.drao.nrc.ca/icarus) are considered.

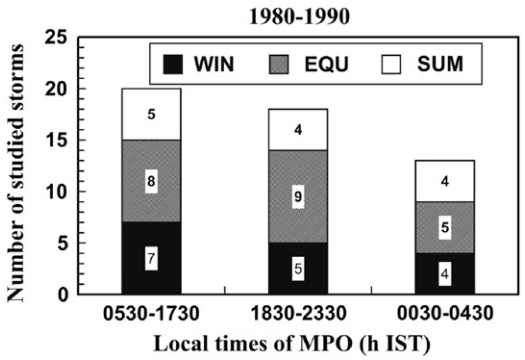

Fig. 1. Distribution of studied severe ($D_{st} \leq -100$ nT) geomagnetic storms during the period of 1980–1990. The numbers within the histograms stand for the number of storms considered in the specific season during the stated MPO intervals. "WIN" indicates local winter solstitial months (November, December and January), "EQU" represents equinoctial months (February, March, April, August, September and October) and "SUM" indicates local summer months (May, June and July).

3. Results

3.1. Occurrences of ESF near the magnetic equator and scintillation near the anomaly crest during severe geomagnetic disturbances

3.1.1. Main phase

For each category of storms, the percentage occurrences of nighttime ESF at Kodaikanal and amplitude scintillation recorded at Calcutta are studied during the main phase of storms. Fig. 2 shows percentage occurrences of ESF and scintillation events categorized on the basis of occurrence times, either in the local premidnight (PREM) (1800–0000 h IST) or postmidnight (POST) (0000–0400 h IST) hours.

The statistical analysis on the occurrence characteristics of ESF at Kodaikanal reveals that for all categories of storms, percentage occurrence of premidnight events is larger than the postmidnight ones. Also, largest percentage occurrences of premidnight (80%) as well as postmidnight (33%) events are recorded for storms with MPO in premidnight time sector (Category 2).

A somewhat similar result is obtained when the occurrence statistics of scintillations from Calcutta are considered. The largest percentage (62%) occurrence of premidnight scintillation is found to be associated with MPO during premidnight hours (Category 2). It may be noted that occurrence of scintillation on the geomagnetically quiet days is mostly a premidnight phenomenon excepting in the local summer months when comparable occurrence of scintillation is also observed during postmidnight hours (Fig. 3). For storms with MPO in the postmidnight local time sector (Category 3) the scintillation in the same time sector is found to be inhibited.

During the following nights and before onset of recovery phase (not shown), a larger percentage occurrence of premidnight ESF events (57%) compared to postmidnight ones (25%) is noted, while nearly equal percentage (~36%) occurrences of scintillation are recorded in the two nighttime sectors (pre and postmidnight) from Calcutta.

3.1.2. Recovery phase

The occurrence statistics of ESF during the recovery phases of each category of storms are shown in Fig. 4 (left panel). In the nighttime sector corresponding to the maximum negative excursion of D_{st} (N0), a larger percentage occurrence of premidnight ESF is recorded for storms with EMP during premidnight hours (Category 2). During postmidnight period of the same night (N0), highest percentage occurrence of ESF is noted for storms with

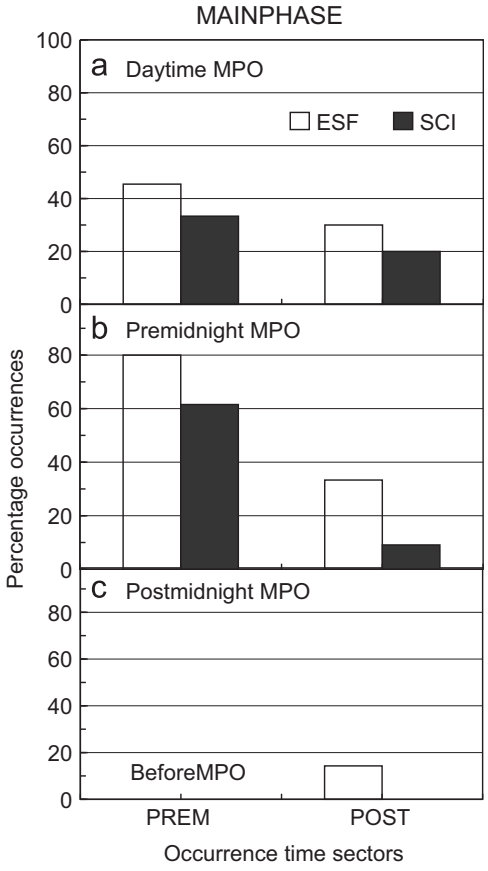

Fig. 2. Histograms showing percentage occurrences of ESF and scintillation (SCI) in the local premidnight (PREM) and postmidnight (POST) sectors during main phase of severe geomagnetic storms classified according to onset times of main phase (MPO) during (a) daytime (0530–1730 h IST)—Category 1, (b) premidnight (1830–2330 h IST)—Category 2 and (c) postmidnight hours (0030–0430 h IST)—Category 3.

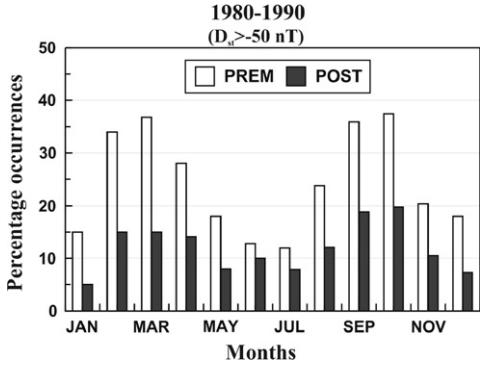

Fig. 3. Monthly percentage occurrences of premidnight (PREM) and postmidnight (POST) scintillations at 136.11 MHz during geomagnetically quiet days ($D_{st} > -50$ nT) of the period 1980–1990.

postmidnight EMP (Category 3). It may be noted that for storms with EMP in the postmidnight hours (Category 3), premidnight period covers the main phase.

The local time effects seem to be very pronounced in the occurrence statistics of scintillation recorded around the anomaly crest region (Fig. 4, right panel). An overall lower occurrence level of scintillation compared to ESF is evident. On night N0, a negligibly low percentage occurrence of scintillation for daytime EMP (Category 1) and an enhanced postmidnight occurrence corresponding to EMP in postmidnight time sector (Category 3)

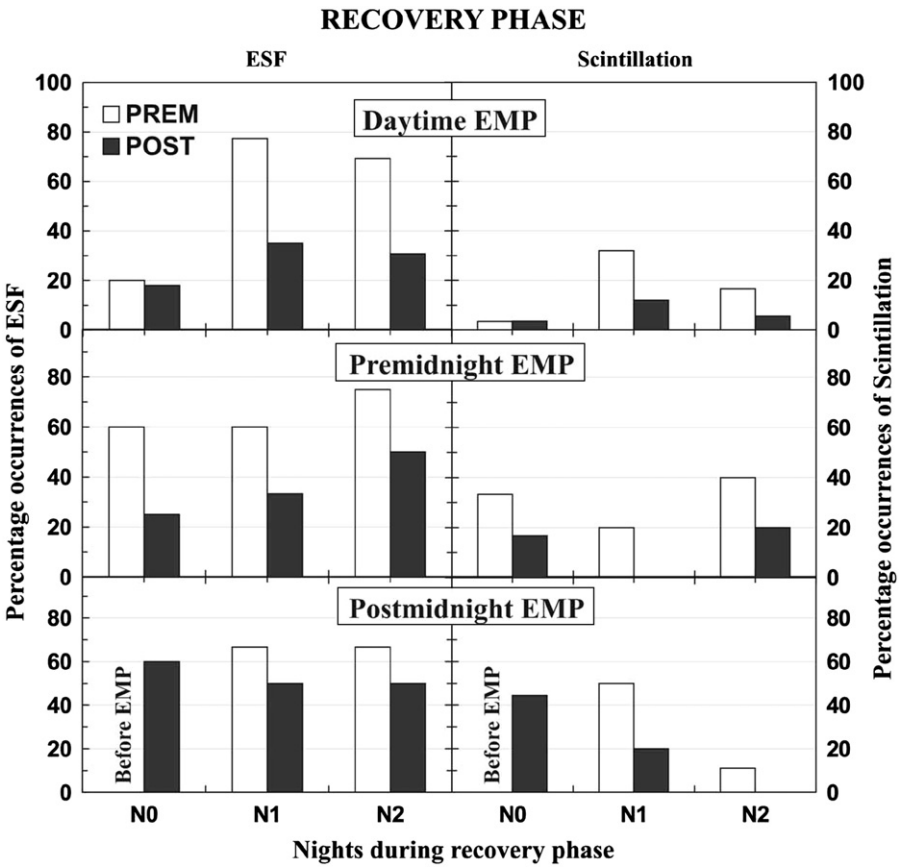

Fig. 4. Histograms exhibiting percentage occurrences of premidnight (PREM) and postmidnight (POST) ESF (left panel) and scintillation (right panel) in the recovery phase of storms categorized on the basis of local time sectors of EMP during (i) daytime (0530–1730 h IST), (ii) premidnight (1830–2330 h IST) and (iii) postmidnight hours (0030–0430 h IST). "N0" represents the night corresponding to maximum negative excursion of D_{st}, "N1" and "N2" correspond to second and third nights of the recovery phase, respectively. For storms with EMP during 0030–0430 h IST the premidnight occurrences in N0 night are not shown as the premidnight sector is within the main phase.

are the remarkable features. The percentage occurrences for storms with EMP during premidnight hours (Category 2) lie in between the above two extreme categories.

Considering the effect of ring current in changing the F-layer height which is considered to be an important parameter for evolution of nighttime irregularities, Aarons (1991) put forward a hypothesis on the local time dependent effect of maximum ring current excursion (D_{st}). Accordingly the maximum negative excursion, as characterized by the D_{st} index, well before height rise of the postsunset F-layer leads to inhibition of irregularities and for maximum negative excursion during postmidnight sector, the F-layer is uplifted after midnight to create favorable conditions for generation of irregularities. For maximum negative excursion of D_{st} in sunset to premidnight sector the layer height, hence irregularity generation, was suggested to exhibit the quiet time patterns. The present results seem to follow more or less the above hypothesis.

The local sunrise and sunset periods are considered to be most critical sectors for observing magnetic storm related perturbation effects because the periods are dominated by sharp changes in conductivity around the solar terminator line. An investigation has been made on the occurrence statistics of scintillation for initiations of main and recovery phases around local sunrise (0330–0530 h IST) and sunset (1730–1930 h IST) periods. For MPO and EMP around the sunset and sunrise times, the scintillation occurrence statistics more or less follow the patterns as reported earlier for Category 2 and Category 3, respectively (Figs. 2 and 4). No remarkable difference in the occurrence statistics is reflected.

On the two consecutive nights (N1 and N2) following N0, appreciable premidnight and postmidnight occurrences of ESF are recorded for all categories of storms. The night N1 is found to be more efficient in exhibiting premidnight scintillation except for Category 2. In the later case larger scintillation occurrences are observed in the night N2.

It may be noted that a complete or partial suppression of irregularities – depending on the severity of storms – during the nights N1 and N2 was reported by Dabas et al. (1989) for all categories of storms. Recent studies based on DMSP data also reported prolonged absence of premidnight irregularities at the altitudes of ~850 km during recovery phases of severe geomagnetic storms (Burke et al., 2009, and references therein). The results of present investigation based on finer details of the occurrences/phases of a large number (51) of severe ($D_{st} \leq -100$ nT) geomagnetic storms seem to deviate from the reported results.

The seasonal features of the percentage occurrences of pre and postmidnight events in different phases of the storms are shown in Fig. 5. It may be noted that during magnetically quiet days the occurrences of nighttime scintillation at Calcutta were reported (DasGupta et al., 1981; Chakraborty et al., 1999) to be primarily equinoctial and local winter solstitial phenomena with negligible occurrences in local summer months. Present study during intense geomagnetic storms reveals that occurrence probabilities of pre and postmidnight events depend intricately on the phases of the storms. For premidnight ESF/scintillation, the maximum and minimum occurrences in main phase are noted during equinoctial and summer solstitial months respectively, similar

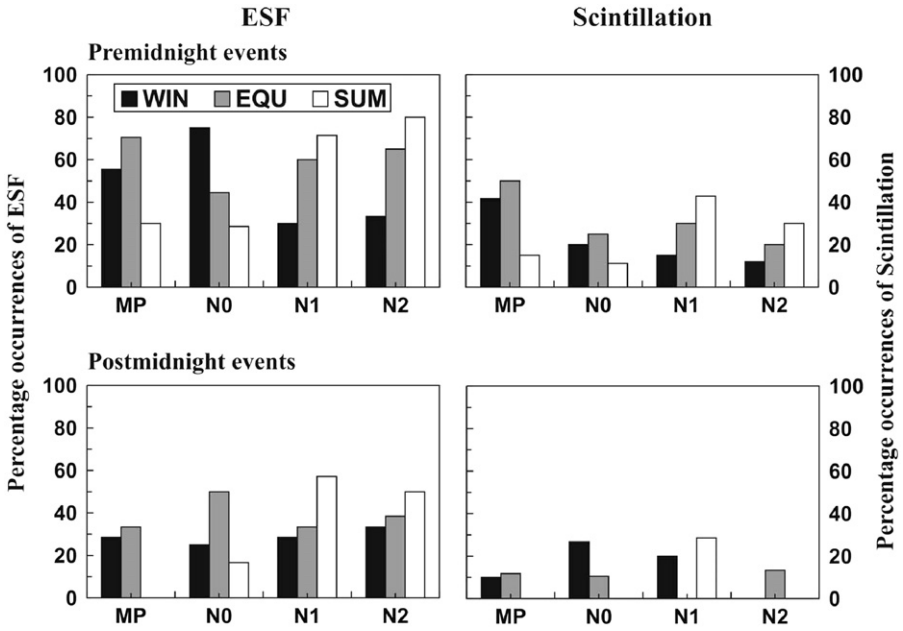

Fig. 5. Histograms showing percentage occurrences of ESF (left panel) and scintillation (right panel) during local winter (WIN), equinox (EQU) and local summer (SUM) months. "MP" indicates main phase of storms.

to the quiet time occurrence pattern. During the night N0, winter solstice replaces the equinoxes for occurrences of premidnight ESF. The occurrence probability of pre and postmidnight events in the following nights (N1 and N2) noticeably increases during summer solstitial months. Thus the suggestions (Chandra et al., 1979; Groves et al., 1997; Becker-Guedes et al., 2004) of (i) triggering of premidnight irregularities during "non-ESF season" and inhibition during "ESF season" and (ii) increases of the postmidnight events during each season under geomagnetically disturbed conditions are not reflected for observations in the main phase and initial stage of recovery phase (N0), except during the consecutive nights (N1, N2) in the recovery phase. In the main phase of the storms as well as during the night N0, no significant deviation from the quiet time seasonal pattern is reflected.

In the context of solar activity variation, the maximum postmidnight ESF occurrence in N0 night is observed during low solar activity years (1984–1986). The occurrence probability in the same period is reduced (23%) during high solar activity years (1980–1981 and 1989–1990). On the other hand, the occurrence of scintillation is negligible in low solar activity years during pre as well as postmidnight hours, while a comparatively higher percentage occurrence (~25%) of scintillation during pre and postmidnight hours of N0 is observed in the high solar activity years. Thus the solar activity dependence of postmidnight ESF during geomagnetic disturbances seems to be a reversal of the quiet time pattern in conformity with earlier reports (Fejer et al., 1999; Hysell and Burcham, 2002). On the contrary, the storm time scintillation occurrences from Calcutta resemble the quiet time pattern (Chakraborty et al., 1999).

3.2. Statistics of ESF near the magnetic equator and scintillation near anomaly crest during geomagnetic disturbances

A statistical analysis has been made on the association of ESF occurring near the magnetic equator (Kodaikanal) and VHF/UHF scintillation recorded near the anomaly crest location (Calcutta) (Fig. 6). A better correspondence between the occurrences of ESF and scintillation is observed in the premidnight period compared to those in the postmidnight sector irrespective of phases of the

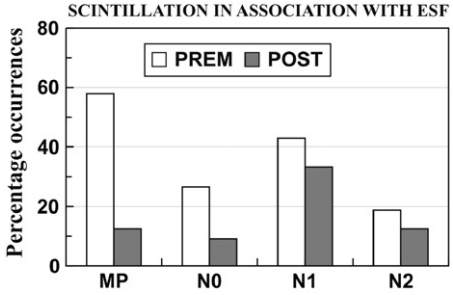

Fig. 6. Histograms showing percentage occurrence of premidnight (PREM) and postmidnight (POST) scintillation events in association with ESF during different phases of magnetic storms. "MP" refers to main phase, "N0" to the night corresponding to maximum negative excursion of D_{st}, "N1" and "N2" are the following nights in the recovery phase.

storms. For premidnight events better correspondence is noted in the main phase than in the recovery phase, while similar phase dependent feature is not always reflected for postmidnight events. In the recovery phase, maximum correspondence is noted during the second night (N1) following maximum negative excursion of D_{st}. On the seasonal basis (not shown), the correspondence during the main phase is found to be more or less same in all the three seasons. In the recovery phase, a greater correspondence is noted for the premidnight events at equinox and postmidnight events during summer. A test of significance reveals a high level of association between the two.

The correspondence between the two phenomena during the periods of geomagnetic disturbances is, thus, largely dependent on the phases of the storm as well as on the local times (pre or postmidnight) of occurrences of the events. The scale sizes of irregularities responsible for ESF and scintillation are different with different life times. Considering the fact that ESF is generated normally around sunset, there should be a difference between the occurrences of ESF and scintillation in the postmidnight period. Moreover, the postmidnight ESF often includes frequency type ESF. The mechanism for generation of this type of ESF is different from that of premidnight one which is of range type. It should be mentioned that ionosonde data available at 1 h interval are used

to identify the signatures of ESF. The non-availability of proper database of ESF with respect to time resolution and type (either range or frequency spread-F) seems to obscure the proper association analysis.

A comparative study on the storm induced scintillation features at two frequencies (136.11 and 244 MHz) reveals that for simultaneous observations, scintillation initiates earlier in 77% cases and have longer duration in 83% cases on ETS-2 path compared to that of FSC. The scale sizes of irregularities causing scintillations at 136.11 (~1.2 km) and 244 MHz (~800 m) are different. Irregularities of shorter scale size are generated little later and have smaller power. The earlier occurrences of scintillation in ETS-2 path in majority of cases may also be the signatures of westward drift of irregularity (Aarons and DasGupta, 1984; Groves et al., 1997; Basu et al., 2005) while larger scale size of irregularities at 136.11 MHz have slower decay time (Basu and Basu, 1981). It may be noted that during magnetically quiet days, westward irregularity drift at the equatorial latitudes in the initial stages of irregularity generation and eastward drift after the development of irregularities were reported from earlier studies (Rastogi et al., 1990). On the other hand, during the period of intense storms, westward irregularity drifts were reported at dawn (Aarons and DasGupta, 1984) as well as at dusk (Basu et al., 2005) from EIA crest location and also from location near the magnetic equator (Groves et al., 1997). Basu et al. (1996) reported eastward irregularity drift near the magnetic equator accompanied by westward drift near the anomaly peak using the scintillation measurements during magnetic storm. The westward drift may be attributed to the effect of storm time equatorward neutral wind – effective within ~2–4 h after storm onset (Tsurutani et al., 2008) – that turns westward under the action of the Coriolis force (Richmond and Lu, 2000).

During period of simultaneous observations of transionospheric signals from ETS-2 and FSC, 11 cases are noted when scintillation was recorded in the path of ETS-2, but not in the path of FSC. The reverse phenomenon is true in 8 cases. Out of 11 cases of observing scintillation in ETS-2 path, ionosonde data are available for 10 days and 6 days of scintillation occurrence are found to be associated with ESF. On the other hand, out of 8 cases of scintillation in FSC path, ionosonde data for one day is not available. Of the remaining 7 scintillation events, occurrences on 4 days are not associated with ESF. The scintillations recorded in a single satellite path on 8 days in absence of ESF may be attributed to the magnetic storm related locally generated irregularities which may not have sufficient lifetime to reach the path of other satellite for producing scintillation or have drifted in another direction. It may be noted that longitudinal separation between the two satellite paths is ~5° with 400 km sub-ionospheric point of ETS-2 path being located east of FSC. The occurrence of scintillation in a particular satellite path may be the signature of longitudinal confinement of magnetic storm related irregularities or coexistence of stable and unstable ionospheres with a longitude separation of 5° (Aarons and DasGupta, 1984; Basu et al., 1996, 2005). It may be mentioned that no specific dependence on local time (either pre or postmidnight) or phases (main or recovery) of magnetic storm is observed for non-occurrence of scintillation in either satellite path.

3.3. Scintillation in relation to nighttime ambient level near the anomaly crest location

Intensification of the EIA around the sunset hours was suggested (Raghavarao et al., 1988; Valladares et al., 2001) to be associated with the onset of ESF/scintillation under quiet geomagnetic conditions. From Calcutta persistence of high ambient ionization and injection of irregularities in the post-sunset period under geomagnetically quiet conditions were reported to be conducive for intense scintillation activity (Chakraborty et al., 1999).

A statistical analysis is made to relate the changes in ambient level near the anomaly crest with occurrence of scintillation during sunset to premidnight period (1800–0000 h IST) under geomagnetically active condition. For this, the deviations of diurnal TEC from quiet days' mean values are estimated and amplitudes of TEC deviations in the postsunset period are studied. It is observed that (i) during the postsunset period a lower ambient level compared to the average one is always associated with the non-occurrence of scintillation, (ii) for ambient level higher than the average one, the triggering or inhibition of scintillation depends on the initiation times of positive deviation as well as amplitudes of TEC enhancement in the postsunset period preceding the scintillation events.

During equinoctial months of high solar activity years (1980–1981 and 1989–1990) it is noted (Fig. 7) that for initiation of positive deviation later than 1900 h IST, the enhancement amplitude must be higher than 30 TEC units for occurrence of scintillation. On the contrary, for earlier initiation of TEC enhancement the postsunset scintillation occurrence is found to be present for a wide range of enhancements.

3.4. Virtual height of F-layer near the magnetic equator in relation to ESF and scintillation occurrences

The height of the F-layer base (h′F) at night is assumed to be the single most important parameter for the generation of irregularities (Farley et al., 1970; Fejer et al., 1999).

In the present analysis the threshold values of the virtual height of F-layer (h′F) for observing ESF at the magnetic equator (Kodaikanal) and scintillation near anomaly crest (Calcutta) are studied. The threshold values for occurrence of ESF exhibit an increasing trend with solar flux (Fig. 8)—a feature similar to that reported during quiet geomagnetic conditions (Hysell and Burcham, 2002; Chapagain et al., 2009). A variation of threshold values in the range 280–300 km is noted for changes in $F_{10.7}$ in the range 70–200 units for observing ESF. For higher solar flux values, a decreasing trend or saturation-like feature is prominent. The correspondence is not so clear for occurrence of scintillation, rather a scattered nature of the data points is observed. A variation of threshold height in the range 370–440 km at the magnetic equator corresponding to solar flux variation of

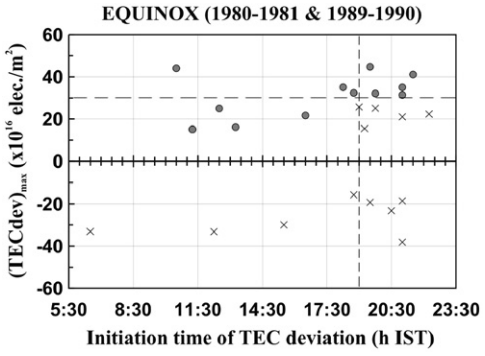

Fig. 7. Maximum TEC deviations, (TEC_{dev})max, in the postsunset period and local times (h IST) of initiations of deviations for occurrences (represented by filled circles) and non-occurrences (represented by crosses) of premidnight scintillations during equinoctial months of high solar activity years (1980–1981, 1989–1990). A threshold value of 30 TEC units (horizontal dashed line) of deviations may be suggested for occurrence of premidnight scintillation when positive TEC deviations initiate after 1900 h IST (vertical dashed line).

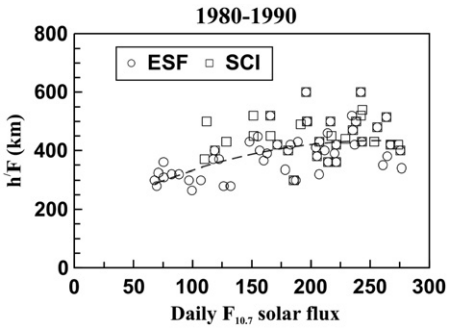

Fig. 8. Solar flux ($F_{10.7}$) variations of virtual height of F-layer (h′F) preceding the occurrence of ESF (circles) and scintillation (squares) during severe geomagnetic storms for the period (1980–1990). The dotted line indicates a non-linear (second order) fit related to occurrence of ESF.

100–250 units may, however, be suggested for occurrence of scintillation at the present location. The threshold value for observing scintillation near anomaly crest is somewhat higher than that for onset of ESF. Occurrence of equatorial scintillation near the anomaly crest is conditioned by the sufficient height rise (~700 km) of the irregularities near the magnetic equator to map down along the magnetic field lines to the sub-ionospheric altitude (400 km) of the observing station. The variability in threshold values seems to increase with solar flux. It may be mentioned that under geomagnetically quiet condition, the threshold of h′F for ESF and scintillation occurrences was reported (Jayachandran et al., 1993; Dabas et al., 2007) to vary in the range 350–450 km for solar flux variation of 70–200 units from low latitude zones. An overall reduction in the threshold values of h′F for triggering of nighttime irregularities under geomagnetically disturbed condition compared to those reported for quiet days is reflected. It may be attributed to the reduction of the postsunset vertical drifts caused by magnetic activity (Fejer et al., 1999; Lee et al., 2005). On seasonal basis, the lowest threshold values are noted during winter solstitial months.

4. Discussions

The basic mechanism for evolution of ESF/plasma density irregularities responsible for scintillation is suggested to be the generalized Rayleigh–Taylor (R–T) instability operating at the bottomside of the F-layer followed by a hierarchy of other instabilities (Haerendel, 1973; Sultan, 1996). The growth rate of instability is mainly controlled by eastward zonal electric field at the magnetic equator and neutral wind system. During geomagnetic disturbances both the factors are intricately modified. The storm time modifications of equatorial electric field are mainly controlled by the relative contributions of prompt penetration (PP) component of magnetospheric origin and ionospheric disturbance dynamo (DD) (Maruyama et al., 2005), which have different local time dependences (Fejer and Scherliess, 1995, 1997; Scherliess and Fejer, 1997). On the other hand, high latitude energy deposition during geomagnetic storms results in (i) westward turning of zonal wind and (ii) strengthening of meridional wind at night (Maruyama et al., 2005; Emmert et al., 2008; Wang et al., 2008), both of which have stabilizing effects on the low latitude ionosphere leading to inhibition of irregularity. The competitive effects of the equatorial electric field and wind system may determine the occurrence probability of ESF and scintillation, in the context of the temporal evolutions of the main and recovery phases of the geomagnetic storms.

According to the empirical model of disturbed time equatorial plasma drift (electric field) proposed by Fejer and Scherliess (1995, 1997) and Scherliess and Fejer (1997) (to be mentioned hereafter as FS model), premidnight storm onset corresponds to upward drift perturbation at the magnetic equator due to direct penetration of magnetospheric electric field in "undershielding" condition. The upward drift perturbation raises the F-layer to high altitudes where conditions favorable for generation of irregularities are obtained. On the other hand, postmidnight storm onset corresponds to large downward drift perturbation that may inhibit the postmidnight irregularities. The present observations of (i) the largest percentage occurrences of premidnight ESF and scintillation for MPO in premidnight sector, and (ii) the negligible occurrence of postmidnight events for MPO during postmidnight period (Fig. 2) are found to be consistent with equatorial drift perturbation (FS model).

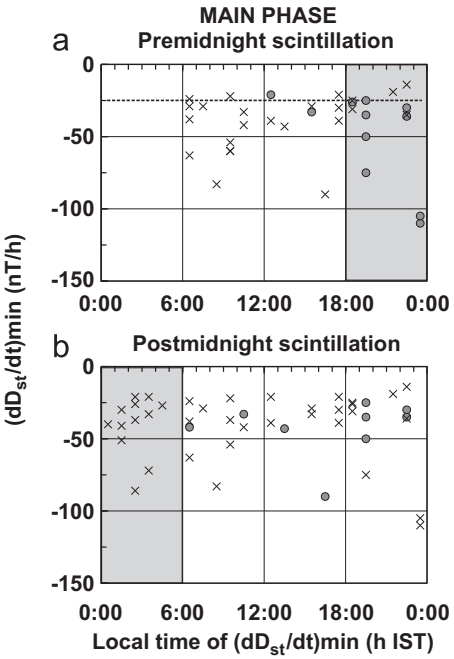

Fig. 9. Local time (h IST) variation of minimum values of dD_{st}/dt (nT/h) in the main phase for (a) premidnight and (b) postmidnight scintillation events. The shaded regions in panels (a) and (b) denote the premidnight and postmidnight occurrences of (dD_{st}/dt)min, respectively. The filled circles represent the occurrences of scintillation while the crosses represent non-occurrences of the same.

Further, during the main phase, rapid changes in D_{st} during local premidnight hours are suggested to be proxy indices for triggering ionospheric irregularity due to eastward PP electric field (Basu et al., 2001; Huang et al., 2002; Tulasi Ram et al., 2008). In the present investigation the evolution/inhibition of scintillation around the anomaly crest is studied in the context of the rate of change/steepest slope of D_{st} (minimum values of dD_{st}/dt) in different local time sectors (Fig. 9). For rapid D_{st} variation in the local premidnight period, scintillation events are found to be largely populated in the same time sector (Fig. 9a), while inhibition of postmidnight events for rapid D_{st} variation during postmidnight sector is also evident (Fig. 9b). From the present investigation a threshold value of $dD_{st}/dt \sim -25$ nT/h during dusk sector may be suggested for observing scintillation from Calcutta.

Depending on the local times of initiation of recovery phase/EMP a remarkable variability in the occurrence statistics of ESF and scintillation is recorded in the night N0 (Fig. 4). It is observed that (i) for EMP during daytime hours, the ESF occurrence is largely reduced and scintillation near the anomaly crest is almost inhibited throughout the night, while (ii) postmidnight events for EMP in the postmidnight local time sector are found to be largely

populated. The late night generation of irregularity was suggested to be related to the anomalous reversal of the nighttime drifts from downward to upward direction under magnetically disturbed condition (Rastogi and Aarons, 1980; Fejer and Emmert, 2003).

In view of the enhanced energy deposition into the high latitude ionosphere during the main or driving phase of the storms, the recovery phase may be under the action of DD related electric field. The polarity of the field is eastward in night (Abdu et al., 2007) with the largest amplitudes during postmidnight hours (FS model). The present result showing negligible occurrences of nighttime (N0) irregularities for EMP during daytime hours (Category 1) may indicate relative dominance of normally prevailing nighttime westward electric field over the DD field. Further, the modification of the nighttime neutral winds in the recovery phase, i.e., the westward change of zonal wind and strengthening of meridional wind (Maruyama et al., 2005; Emmert et al., 2008; Wang et al., 2008) may have some contribution through the stabilization effect leading to inhibition of irregularities.

Around the time of EMP abrupt changes (large decrease followed by increase) in D_{st} normally take place. The importance of abrupt changes in D_{st} to indicate PP effect was suggested by several workers (Ridley and Liemohn, 2002; Martinis et al., 2005). In the present investigation, the probability of occurrence/inhibition of scintillation during the recovery phase is studied in conjunction with the abrupt increase in D_{st} following the onset of recovery phase (Fig. 10). For daytime sharp increase of D_{st}, premidnight (1 out of 30 cases) as well as postmidnight (2 out of 30 cases) scintillation events are negligible. The occurrence probability of postmidnight scintillation increases noticeably (5 out of 10 cases) for sharp increase in D_{st} during postmidnight time sector (Fig. 10b). It may be mentioned that 5 scintillation events during postmidnight period are associated with sudden turning of IMF B_z from southward to northward direction (with $dB_z/dt \sim 3$ nT/min). In the remaining 5 cases for which no postmidnight scintillation is observed in spite of sharp D_{st} increase during postmidnight sector, the simultaneous northward turning of IMF B_z was absent. An abrupt northward turning of IMF B_z is related to the nighttime eastward perturbation of equatorial electric field due to a direct penetration of the interplanetary electric field (Kelley et al., 1979). During initiation of recovery phase in the postmidnight period an abrupt increase in D_{st} in conjunction with sharp northward turning of IMF B_z may, thus, be related to penetration of eastward electric field leading to generation of equatorial irregularities. Further, according to FS model, recovery onset (indicated by sharp fall in AE index) after midnight period results in large upward drift perturbation during postmidnight to predawn local time sector due to combined effects of "overshielding" eastward PP electric field and the eastward DD electric field. The mechanism may explain the enhanced probability of postmidnight irregularities for EMP during the same time sector (Fig. 4). On the other hand, a large downward drift perturbation during the premidnight sector for EMP in the premidnight hours is predicted by the model (FS). It may inhibit the premidnight irregularity processes. The corresponding postmidnight period may be associated with upward drift perturbations due to DD effect. The result of reduced probability of irregularity generation during the postmidnight period – well inside the recovery phase – compared to corresponding premidnight sector (Fig. 4), seems not to comply with the model (FS) prediction of drift perturbation. The suppression of the irregularity processes may indicate the dominance of stabilizing effects of the storm time disturbance winds. For postsunset maximum excursion of D_{st}, strengthening of meridional wind and westward change in zonal wind take place most effectively during postmidnight period (Maruyama et al., 2005; Emmert et al., 2008; Wang et al., 2008), both of which may stabilize the ionosphere and reduce the irregularity activities.

The variability in occurrences of ESF and scintillation during consecutive nights (N1, N2) after EMP may be related to long-term effects of DD (Scherliess and Fejer, 1997) having their origin in storm related composition/conductivity changes (Fuller-Rowell et al., 1996), which drives upward drift perturbation at night.

For observing equatorial scintillation near the anomaly crest, injection of equatorial irregularities in an environment of high ambient ionization is the prerequisite. The severity of scintillation is proportional to the height-integral of the product of irregularity amplitude and the ionization density along the ray path (Basu et al., 1996). Around postsunset period low values of electron density – which are omnipresent in low solar activity periods – may lead to inhibition of scintillation, while occurrences and maintenance of positive ionospheric storm effect for a long period may provide suitable conditions conducive for scintillation. Further, for observing scintillation near the anomaly crest, equatorial plasma bubble related irregularities are required to rise to a sufficiently high altitude for mapping down to the anomaly crest locations. If the irregularity structures generated at the magnetic equator in form of thin layer are unable to be lifted to sufficiently high altitude, no footprint may be observed at the anomaly crest location. In addition, lower strength/less population and drift/fast decay of irregularities of specific scale sizes generated at the magnetic equator may lead to non-availability of the same near the anomaly crest location. The constraints may contribute to the lower percentage occurrence of scintillation near the crest location compared to the evolution of ESF at the magnetic equator.

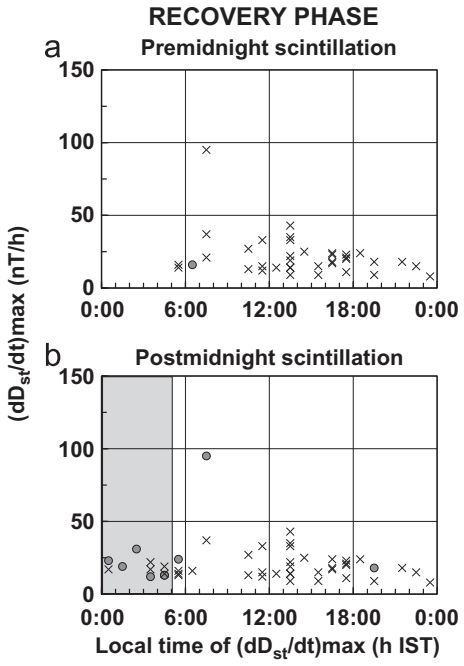

Fig. 10. Local time (h IST) variation of dD_{st}/dt (nT/h) following the onset of recovery phase of the storms. Filled circles represent the occurrences of scintillation while crosses refer to non-occurrences of the same during (a) premidnight and (b) postmidnight local time sectors. The shaded region in panel (b) shows the postmidnight occurrences of dD_{st}/dt.

5. Summary and conclusions

The results of studies on the variability of the ionospheric scintillation and ESF during a large number (51) of intense

geomagnetic storms distributed over a period of one solar cycle (1980–1990) may be summarized as follows:

1. During main phase of geomagnetic storms the important features are the high percentage occurrences of premidnight ESF and scintillation for MPO in the premidnight sector and negligible occurrences of postmidnight events for MPO during postmidnight hours (Fig. 2).
2. In the main phase a rapid decrease in D_{st} index at the rate $dD_{st}/dt \leq \sim -25$ nT/h in dusk sector may be suggested as a proxy index for occurrence of premidnight scintillations near the anomaly crest (Fig. 9).
3. On the night corresponding to maximum negative excursion of D_{st} (N0), the occurrences of ESF and scintillation are significantly reduced for EMP during daytime hours, while triggering of the postmidnight events may be accentuated for EMP in postmidnight sector (Fig. 4).
4. During initial stages of main and recovery phases, the generation/inhibition of irregularities seems to comply well with the modifications of equatorial electric fields/drift perturbations as predicted by the FS model. The storm time modification of neutral wind system at night seems to play a significant role in (i) the reduction in probability of postmidnight irregularity generation compared to premidnight for EMP in the premidnight sector and (ii) prominent suppression of nighttime irregularities for daytime EMP (Fig. 4).
5. In the recovery phase, an abrupt increase in D_{st} in conjunction with sudden northward turning of IMF B_z in the local postmidnight sector may also be a proxy for triggering of postmidnight scintillation (Fig. 10).
6. During the second (N1) and third (N2) nights following the onset of recovery phase, summer solstitial months are found to exhibit increased occurrences of irregularities compared to other seasons (Fig. 5).
7. While lower ambient density level compared to the quiet time average near the anomaly crest at premidnight is always associated with inhibition of scintillation, triggering of the same depends on the magnitudes and initiation times of enhancement. For initiation of positive deviation in TEC after 1900 h IST in high solar activity years, a threshold increase of 30 TEC units may be suggested for occurrence of scintillation, while earlier initiation of TEC enhancements may be the precursor for magnetic storm related scintillation occurrence though no threshold value of TEC deviation may be inferred (Fig. 7).
8. During the period of magnetic disturbances, the threshold value of virtual height of F-layer (h′F) necessary for generation of ESF is found to increase with solar flux and a saturation-like feature is revealed at higher solar flux levels ($F_{10.7} > 200$ units) (Fig. 8).
9. For observing equatorial irregularities, a reduction in threshold values of h′F during magnetically active condition compared to those reported for quiet time period is reflected.

The results of investigations thus accrued may form an important database for the development of equatorial ionospheric model during geomagnetically disturbed conditions and may be useful for space weather prediction.

Acknowledgments

The work has been carried out with the financial assistance of Indian Space Research Organization under the RESPOND Program. Authors are also thankful to Prof. J.H. Sastri, IIA, Bangalore, for providing ionosonde data.

References

Aarons, J., 1991. The role of the ring current in the generation or inhibition of equatorial F layer irregularities during magnetic storms. Radio Science 26, 1131–1149.
Aarons, J., DasGupta, A., 1984. Equatorial scintillations during the major magnetic storm of April 1981. Radio Science 19, 731–739.
Abdu, M.A., Maruyama, T., Batista, I.S., Saito, S., Nakamura, M., 2007. Ionospheric response to the October 2003 superstorm: longitude/local time effects over equatorial low and middle latitudes. Journal of Geophysical Research 112, A10306. doi:10.1029/2006JA012228.
Abdu, M.A., Batista, I.S., Reinisch, B.W., Souza, J.R., Sobral, J.H.A., Pedersen, T.R., Medeiros, A.F., Schuch, N.J., de Paula, E.R., Groves, K.M., 2009. Conjugate point equatorial experiment (COPEX) campaign in Brazil: electrodynamics highlights on spread F development conditions and day-to-day variability. Journal of Geophysical Research 114, A04308. doi:10.1029/2008JA013749.
Anderson, D., Haerendel, G., 1979. The motion of depleted plasma regions in the equatorial ionosphere. Journal of Geophysical Research 84, 4251–4256.
Basu, S., Basu, Su., 1981. Equatorial scintillation—a review. Journal of Atmospheric and Terrestrial Physics 43, 473–489.
Basu, S., Kudeki, E., Basu, Su., Valladares, C.E., Weber, E.J., Zengingonul, H.P., Bhattacharyya, S., Sheehan, R., Meriwether, J.W., Biondi, M.A., Kuenzler, H., Espinoza, J., 1996. Scintillations, plasma drifts, and neutral winds in the equatorial ionosphere after sunset. Journal of Geophysical Research 101, 26795–26809.
Basu, Su., Basu, S., Valladares, C.E., Yeh, H.-C., Su, S.-Y., MacKenzie, E., Sultan, P.J., Aarons, J., Rich, F.J., Doherty, P., Groves, K.M., Bullett, T.W., 2001. Ionospheric effects of major magnetic storms during the International Space Weather Period of September and October 1999: GPS observations, VHF/UHF scintillations, and in situ density structures at middle and equatorial latitudes. Journal of Geophysical Research 106, 30389–30413.
Basu, S., Groves, K.M., Basu, Su., Sultan, P.J., 2002. Specification and forecasting of scintillations in communication/navigation links: current status and future plans. Journal of Atmospheric and Solar-Terrestrial Physics 64, 1745–1754.
Basu, S., Basu, Su., Groves, K.M., MacKenzie, E., Keskinen, M.J., Rich, F.J., 2005. Near-simultaneous plasma structuring in the midlatitude and equatorial ionosphere during magnetic superstorms. Geophysical Research Letters 32, L12S05. doi:10.1029/2004GL021678.
Becker-Guedes, F., Sahai, Y., Fagundes, P.R., Lima, W.L.C., Pillat, V.G., Abalde, R., Bittencourt, J.A., 2004. Geomagnetic storm and equatorial spread-F. Annales Geophysicae 22, 3231–3239.
Biktash, L.Z., 2004. Role of the magnetospheric and ionospheric currents in the generation of the equatorial scintillations during geomagnetic storms. Annales Geophysicae 22, 3195–3202.
Burke, W.J., Huang, C.Y., Sharma, R.D., 2009. Stormtime dynamics of the global thermosphere and equatorial ionosphere. Annales Geophysicae 27, 2035–2044.
Chakraborty, S.K., DasGupta, A., Ray, S., Banerjee, S., 1999. Long-term observations of VHF scintillation and total electron content near the crest of the equatorial anomaly in the Indian longitude zone. Radio Science 34, 241–255.
Chandra, H., Vyas, G.D., Rastogi, R.G., 1979. On the relationship between magnetic activity and spread-F at Huancayo. Annales Geophysicae 35, 11–14.
Chapagain, N.P., Fejer, B.G., Chau, J.L., 2009. Climatology of postsunset equatorial spread F over Jicamarca. Journal of Geophysical Research 114, A07307. doi:10.1029/2008JA013911.
Cohen, R., Bowles, K., 1961. On the nature of equatorial spread F. Journal of Geophysical Research 66, 1081–1106.
Dabas, R.S., Lakshmi, D.R., Reddy, B.M., 1989. Effect of geomagnetic disturbances on the VHF nighttime scintillation activity at equatorial and low latitudes. Radio Science 24, 563–573.
Dabas, R.S., Das, R.M., Sharma, K., Garg, S.C., Devasia, C.V., Subbarao, K.S.V., Niranjan, K., Rama Rao, P.V.S., 2007. Equatorial and low latitude spread-F irregularity characteristics over the Indian region and their prediction probabilities. Journal of Atmospheric and Solar-Terrestrial Physics 69, 685–696.
DasGupta, A., Maitra, A., Basu, S., 1981. Occurrence of nighttime VHF scintillations near the equatorial anomaly crest in the Indian sector. Radio Science 16, 1455–1458.
DasGupta, A., Maitra, A., Das, S.K., 1985. Post-midnight equatorial scintillation activity in relation to geomagnetic disturbances. Journal of Atmospheric and Terrestrial Physics 47, 911–916.
Emmert, J.T., Drob, D.P., Shepherd, G.G., Hernandez, G., Jarvis, M.J., Meriwether, J.W., Niciejewski, R.J., Sipler, D.P., Tepley, C.A., 2008. DWM07 global empirical model of upper thermospheric storm-induced disturbance winds. Journal of Geophysical Research 113, A11319. doi:10.1029/2008JA013541.
Farley, D.T., Balsley, B.B., Woodman, R.F., McClure, J.P., 1970. Equatorial spread F: implications of VHF radio observations. Journal of Geophysical Research 75, 7199–7216.
Fejer, B.G., Emmert, J.T., 2003. Low latitude ionospheric disturbance electric field effects during the recovery phase of the 19–21 October 1998 magnetic storm. Journal of Geophysical Research 108, A121454. doi:10.1029/2003JA010190.
Fejer, B.G., Scherliess, L., 1995. Time dependent response of equatorial ionospheric electric fields to magnetospheric disturbances. Geophysical Research Letters 22, 851–854.
Fejer, B.G., Scherliess, L., 1997. Empirical models of storm time equatorial zonal electric fields. Journal of Geophysical Research 102, 24047–24056.

Fejer, B.G., Scherliess, L., de Paula, E.R., 1999. Effects of the vertical plasma drift velocity on the generation and evolution of equatorial spread F. Journal of Geophysical Research 104, 19859–19869.

Fuller-Rowell, T.J., Codrescu, M.V., Rishbeth, H., Moffett, R.J., Quegan, S., 1996. On the seasonal response of the thermosphere and ionosphere to geomagnetic storms. Journal of Geophysical Research 101, 2343–2353.

Groves, K.M., Basu, S., Weber, E.J., Smitham, M., Kuenzler, H., Valladares, C.E., Sheehan, R., MacKenzie, E., Secan, J.A., Ning, P., McNeill, W.J., Moonan, D.W., Kendra, M.J., 1997. Equatorial scintillation and system support. Radio Science 32, 2047–2064.

Haerendel, G., 1973. Theory of Equatorial Spread F. report, Max-Planck Inst. Fur Phys. and Astrophys., Munich.

Haerendel, G., Eccles, V., Cakir, S., 1992. Theory for modeling the equatorial evening ionosphere and the origin of the shear in the horizontal plasma flow. Journal of Geophysical Research 97, 1209–1223.

Huang, C., Burke, W., Machuzak, J., Gentile, L., Sultan, P.J., 2002. Equatorial plasma bubbles observed by DMSP satellites during a full solar cycle: toward a global climatology. Journal of Geophysical Research 107, 1434. doi:10.1029/2002JA009452.

Hysell, D.L., Burcham, J.D., 2002. Long term studies of equatorial spread F using the JULIA radar at Jicamarca. Journal of Atmospheric and Solar-Terrestrial Physics 64, 1531–1543.

Jayachandran, B., Balan, N., Rao, P.B., Sastri, J.H., Bailey, G.J., 1993. HF Doppler and ionosonde observations on the onset conditions of equatorial spread F. Journal of Geophysical Research 98, 13741–13750.

Kelley, M.C., Fejer, B.G., Gonzales, C.A., 1979. An explanation for anomalous equatorial ionospheric electric fields associated with a northward turning of the interplanetary magnetic field. Geophysical Research Letters 6, 301–304.

Kelley, M.C., Larsen, M.F., LaHoz, C., 1981. Gravity wave initiation of equatorial spread F: a case study. Journal of Geophysical Research 86, 9087–9100.

Kil, H., Heelis, R., 1998. Equatorial density irregularity structures at intermediate scales and their temporal evolution. Journal of Geophysical Research 103, 3969–3981.

Kumar, S., Chandra, H., Sharma, S., 2005. Geomagnetic storms and their ionospheric effects observed at the equatorial anomaly crest in the Indian region. Journal of Atmospheric and Solar-Terrestrial Physics 67, 581–594.

Lee, C.C., Liu, J.Y., Reinisch, B.W., Chen, W.S., Chu, F.D., 2005. The effects of the pre-reversal drift, the EIA asymmetry, and magnetic activity on the equatorial spread F during solar maximum. Annales Geophysicae 23, 745–751.

Martinis, C.R., Mendillo, M.J., Aarons, J., 2005. Toward a synthesis of equatorial spread F onset and suppression during geomagnetic storms. Journal of Geophysical Research 110, A07306. doi:10.1029/2003JA010362.

Maruyama, N., Richmond, A.D., Fuller-Rowell, T.J., Codrescu, M.V., Sazykin, S., Toffoletto, F.R., Spiro, R.W., Millward, G.H., 2005. Interaction between direct penetration and disturbance dynamo electric fields in the storm-time equatorial ionosphere. Geophysical Research Letters 32, L17105. doi:10.1029/2005GL023763.

McClure, J., Singh, S., Bamgboye, D., Johnson, F., Kil, H., 1998. Occurrence of equatorial F region irregularities: evidence for tropospheric seeding. Journal of Geophysical Research 103, 29119–29135.

Raghavarao, R., Nageswararao, M., Sastri, J.H., Vyas, G.D., Sriramarao, M., 1988. Role of equatorial ionization anomaly in the initiation of equatorial spread F. Journal of Geophysical Research 93, 5959–5964.

Rastogi, R.G., Aarons, J., 1980. Nighttime ionospheric radio scintillations and vertical drifts at the magnetic equator. Journal of Atmospheric and Terrestrial Physics 42, 583–591.

Rastogi, R., Mullen, J., MacKenzie, E., 1981. Effect of geomagnetic activity on equatorial radio VHF scintillations and spread F. Journal of Geophysical Research 86, 3661–3664.

Rastogi, R.G., Koparkar, P.V., Pathan, B.M., 1990. Nighttime radio wave scintillations at equatorial stations in Indian and American zones. Journal of Geomagnetism and Geoelectricity 42, 1–10.

Richmond, A.D., Lu, G., 2000. Upper-atmospheric effects of magnetic storms: a brief tutorial. Journal of Atmospheric and Solar-Terrestrial Physics 62, 1115–1127.

Ridley, A.J., Liemohn, M.W., 2002. A model-derived storm time asymmetric ring current driven electric field description. Journal of Geophysical Research 107, A81151. doi:10.1029/2001JA000051.

Sahai, Y., Fagundes, P.R., Abalde, J.R., Pimenta, A.A., Bittencourt, J.A., Otsuka, Y., Rios, V.H., 2004. Generation of large-scale equatorial F-region plasma depletions during low range spread-F season. Annales Geophysicae 22, 15–23.

Scherliess, L., Fejer, B.G., 1997. Storm time dependence of equatorial disturbance dynamo zonal electric fields. Journal of Geophysical Research 102, 24037–24046.

Su, S.-Y., Chao, C.K., Liu, C.H., 2008. On monthly/seasonal/longitudinal variations of equatorial irregularity occurrences and their relationship with the postsunset vertical drift velocities. Journal of Geophysical Research 113, A05307. doi:10.1029/2007JA012809.

Sugiura, M., Chapman, S., 1960. The average morphology of geomagnetic storms with sudden commencement. Abhandlungen der Akademie der Wissenschaften in Gottingen, Mathematisch Physikalische Klasse, Sonderh 4, 53.

Sultan, P.J., 1996. Linear theory and modeling of the Rayleigh-Taylor instability leading to the occurrence of equatorial spread F. Journal of Geophysical Research 101, 26875–26891.

Tsurutani, B.T., Verkhoglyadova, O.P., Mannucci, A.J., Saito, A., Araki, T., Yumoto, K., Tsuda, T., Abdu, M.A., Sobral, J.H.A., Gonzalez, W.D., McCreadie, H., Lakhina, G.S., Vasyliunas, V.M., 2008. Prompt penetration electric fields (PPEFs) and their ionospheric effects during the great magnetic storm of 30–31 October 2003. Journal of Geophysical Research 113, A05311. doi:10.1029/2007JA012879.

Tulasi Ram, S., Rama Rao, P.V.S., Prasad, D.S.V.V.D., Niranjan, K., Gopi Krishna, S., Sridharan, R., Rabindran, S., 2008. Local time dependent response of postsunset ESF during geomagnetic storms. Journal of Geophysical Research 113, A07310. doi:10.1029/2007JA012922.

Valladares, C.E., Basu, S., Groves, K., Hagan, M.P., Hysell, D., Mazzella Jr., A.J., Sheehan, R.E., 2001. Measurement of the latitudinal distributions of total electron content during equatorial spread F events. Journal of Geophysical Research 106, 29133–29152.

Wang, W., Burns, A.G., Wiltberger, M., Solomon, S.C., Killeen, T., 2008. Altitude variations of the horizontal thermospheric winds during geomagnetic storms. Journal of Geophysical Research 113, A02301. doi:10.1029/2007JA012374.

Weber, E., Aarons, J., Johnson, A., 1983. Conjugate studies of an isolated equatorial irregularity region. Journal of Geophysical Research 88, 3175–3180.

Woodman, R.F., LaHoz, C., 1976. Radar observations of F region equatorial irregularities. Journal of Geophysical Research 81, 5447–5466.